

# Gradient Diffusion: Enhancing Multicompartmental Neuron Models for Gradient-Based Self-Tuning and Homeostatic Control

Lennart P. L. Landsmeer<sup>1,2</sup>, Mario Negrello<sup>2</sup>, Said Hamdioui<sup>1</sup>, Christos Strydis<sup>2,1</sup>

<sup>1</sup>Delft Technical University, Quantum and Computer Engineering Department, Delft, The Netherlands

<sup>2</sup>Erasmus Medical Center, Department of Neuroscience, NeurocomputingLab, Rotterdam, The Netherlands

December 2024

## Abstract

Realistic brain models contain many parameters. Traditionally, gradient-free methods are used for estimating these parameters, but gradient-based methods offer many advantages including scalability. However, brain models are tied to existing brain simulators, which do not support gradient calculation. Here we show how to extend –within the public interface of such simulators– these neural models to also compute the gradients with respect to their parameters. We demonstrate that the computed gradients can be used to optimize a biophysically realistic multicompartmental neuron model with the gradient-based Adam optimizer. Beyond tuning, gradient-based optimization could lead the way towards dynamics learning and homeostatic control within simulations.

## Introduction

Building realistic models of the brain requires estimating many unobserved parameters, because the full dynamical system state of the brain is not fully observable: The brain models vary from the simplified to the spatially detailed, biophysically realistic multicompartmental conductance-based models – *realistic* models in short. The parameters to be tuned can be protein concentrations, synaptic connections or homeostatic dynamical behaviour. Realistic mod-

els provide the most insights into biology, among others by linking large-scale behaviour to druggable molecular targets. These highly complex models are tightly bound to the surrounding ecosystem of brain simulation software. However, these models also contain a much higher amount of parameters with non-linear effects, calling for careful tuning of parameters of realistic brain models.

General parameter tuning methods can be divided in gradient-free (zero order) or gradient-based (higher order) tuning methods. Currently, gradient-free methods are the dominant method for tuning realistic brain models using existing brain simulations: manual parameter variation, evolutionary search or randomized search[1, 2, 3, 4]. However, gradient-free optimization techniques are known to suffer from the curse of dimensionality: higher dimensional parameter spaces take exponentially longer to tune. Instead, gradient-based methods do not suffer from this curse of dimensionality, and scale to the tuning of billions of parameters, as exemplified by current large AI models. However, existing brain simulators do not provide gradients in their simulations, making it seemingly impossible to use these methods in the existing ecosystem. As such, one effort to implement gradient-based tuning in realistic brain models built a brain simulator from scratch in the JAX automatic-gradient environment[5]. However, this work is still far from NEURON-level compatibility and most existing brain models are not supported in this format.

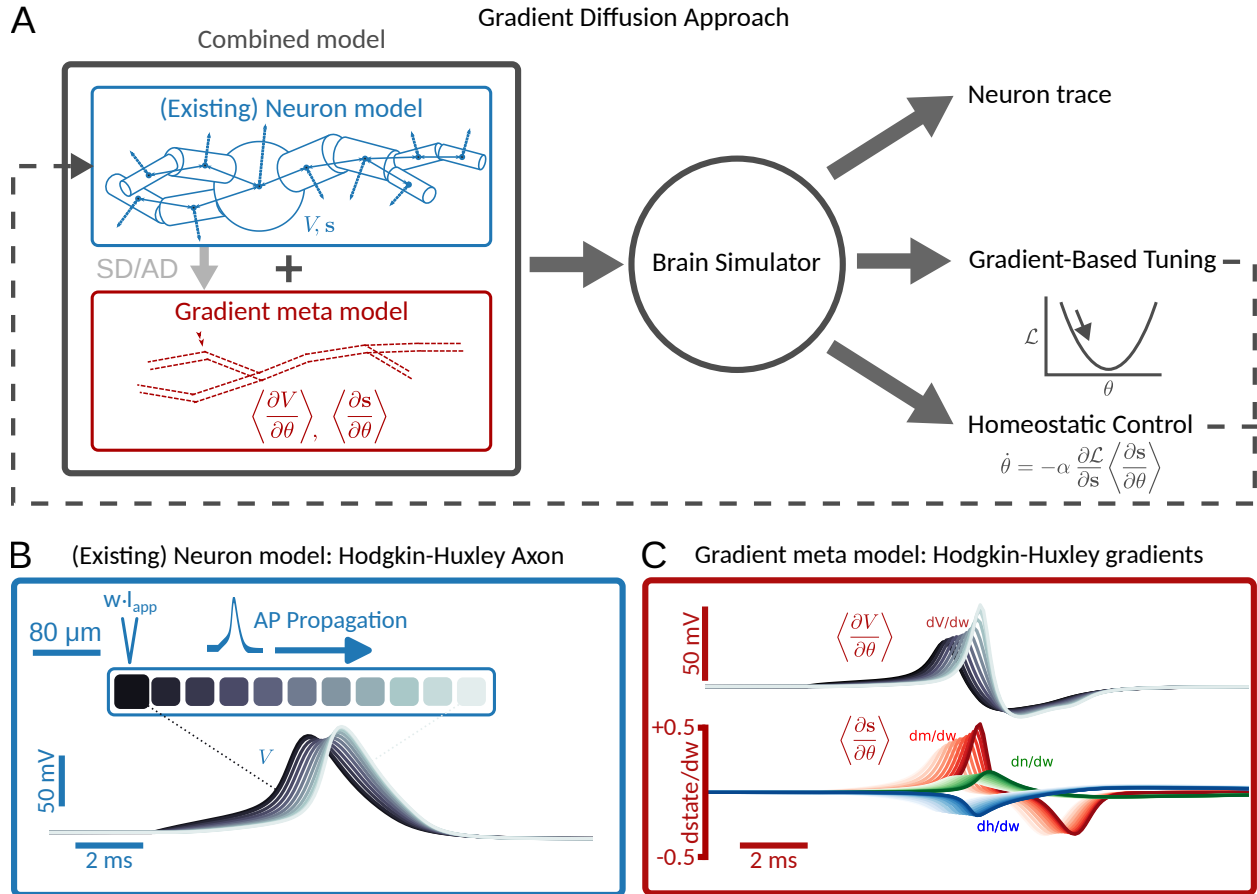


Figure 1: **A** A neuron model is enhanced with a gradient (meta) model, by symbolic or automatic differentiation. This creates a new model, which can be simulated by (existing) brain simulators. Resulting gradients can be used for tuning or homeostatic control, or be useful on their own. The neuron model is a discretized multicompartmental cable cell. Voltage diffusion happens along connected arrows, ion-channel/leak based axial currents flow along dotted arrows. Mechanism state and voltages are maintained at black dots. Such mechanisms, including both state derivatives and transmembrane currents, are written in NMODL files. **B** Hodgkin-Huxley linear axon model, with a pulse current applied on one end to create a propagating action potential (AP). Each compartment has a voltage, which is plotted, showing this propagation. **C** Gradient model of the Hodgkin-Huxley model, showing the resulting gradients over time.

Which raises the question – how could we repurpose existing brain simulators for gradient calculations?

In this article, we describe how to apply gradient-descent based learning and optimization methods in biophysically realistic, morphologically detailed brain models, using existing available brain simulators

## Results

Assume a morphologically detailed biophysically realistic model of a single neuron. At the interface level to the brain simulation software, the modeler essentially defines two functions: The ion-channel current

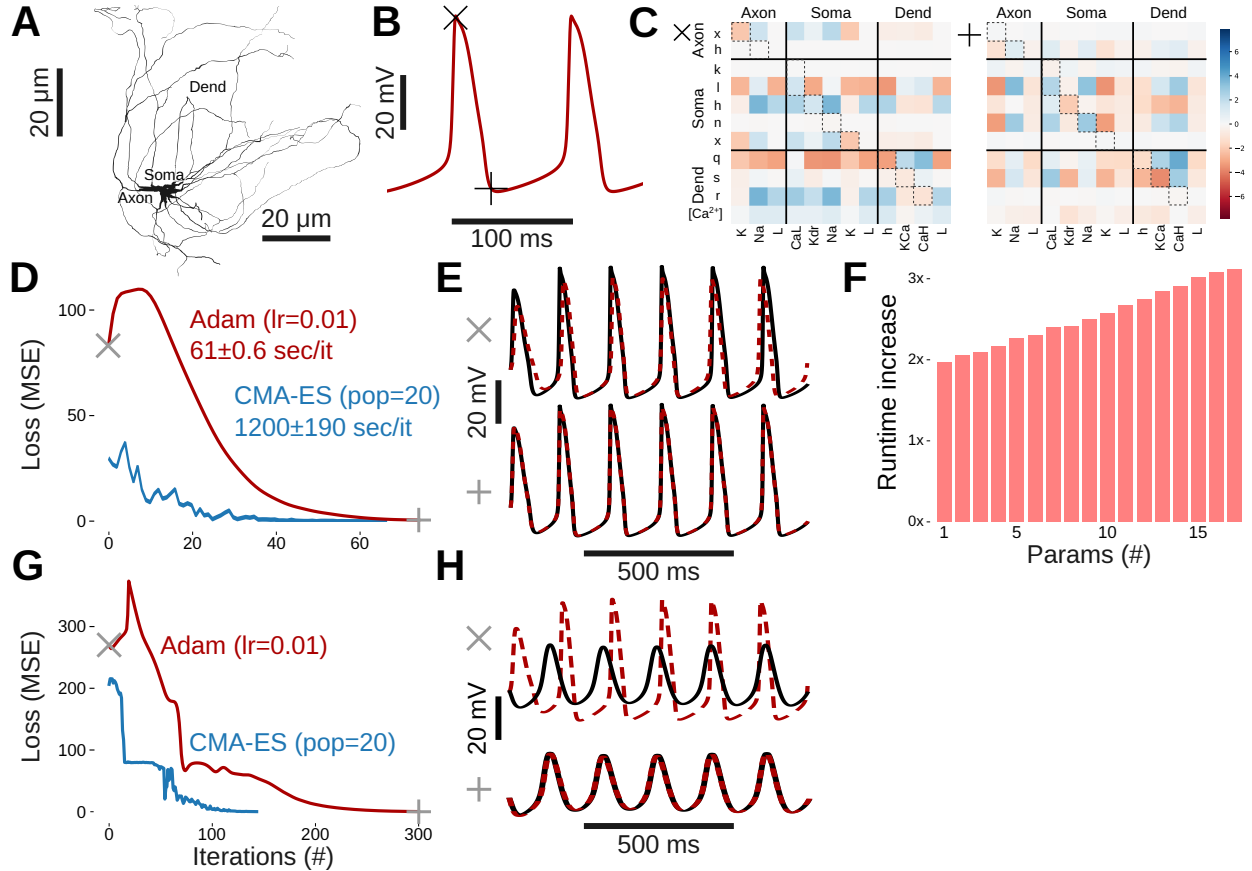


Figure 2: **A**: Simulated neuron morphology **B**: Subthreshold Oscillation (STO) with specific timepoints **C**:  $\langle \frac{\partial s}{\partial \theta} \rangle$  at specific timepoints from **B** **D**, **G**: Loss during optimization using gradient descent (Adam, red) and traditional evolutionary approach (CMA-ES, blue) **E**, **H**: Simulated (red) vs target (black) before (top) and after (bottom) training **F**: Increase in computational time by co-simulation of the gradient system in Arbor

contribution  $i$  to the membrane potential  $V$  (eq. (1)), and the dynamics of the internal state variables  $\mathbf{s}$  (eq. (2)). These function are defined for each position on the spatial neuron and depend on a set of parameters  $\theta$ .

$$i(V, \mathbf{s}, \theta) \quad (1)$$

$$\dot{\mathbf{s}}(V, \mathbf{s}, \theta) \quad (2)$$

The goal is now to find the gradients of the voltage  $V$  and state  $\mathbf{s}$  with respect to the parameters

$\theta$ , at any point in time and for all compartments. To find the gradients, we define a *gradient model*, to be simulated along side the neural model defined in eq. (1) and eq. (2). This gradient model consists of the voltage-gradients  $\langle \frac{\partial V}{\partial \theta} \rangle$  as diffusive ion-species and the state-gradients  $\langle \frac{\partial \mathbf{s}}{\partial \theta} \rangle$  as internal state variables. Here, in our notation, brackets  $\langle \cdot \rangle$  denote new state variables introduced for the simulation of the gradient model. The gradient model calculates the voltage- and state-gradients by direct integration of the sensitivity equation, by supplying their gradients as mechanisms to the brain simulator (see Meth-

ods):

$$\left\langle \frac{\partial \dot{V}}{\partial \theta} \right\rangle \left( V, \mathbf{s}, \theta, \left\langle \frac{\partial V}{\partial \theta} \right\rangle, \left\langle \frac{\partial \mathbf{s}}{\partial \theta} \right\rangle \right) \quad (3)$$

$$\left\langle \frac{\partial \dot{\mathbf{s}}}{\partial \theta} \right\rangle \left( V, \mathbf{s}, \theta, \left\langle \frac{\partial V}{\partial \theta} \right\rangle, \left\langle \frac{\partial \mathbf{s}}{\partial \theta} \right\rangle \right) \quad (4)$$

These time derivatives can be obtained by either symbolic or automatic differentiation. A such, the gradient model can be fully expressed in respectively existing NMODL interfaces (fig. 3) or the autograd-compatible programmatic interface developed in Methods.

## Applications

We now demonstrate the application of gradients in brain models in various use-cases.

**Gradients as Insights** A basic example of calculated gradients is shown in fig. 1B. A linear Hodgkin-Huxley axon is simulated and a current stimulus input. These are implemented in the Arbor NMODL dialect. The weight-derivative, which gates a action-potential creating current, shows similar transient response to the action potential itself. The individual effects on each state variable are also computed during gradient-system simulation.

To show the applicability of the method to more complex models, we applied the method to a 17-parameter model of the Inferior Olivary Nucleus (ION) neuron. The morphology was taken from experimental data (fig. 2A). These neurons show continuous subthreshold oscillators (fig. 2B). The gradient system can give insights in how the interplay between parameters and state give rise to the observed behaviour (fig. 2C).

**Gradient-Based Parameter Tuning** Given a Loss function  $\mathcal{L}(V, \mathbf{s})$ , we can define gradient descent as

$$\theta \leftarrow \theta - \alpha \frac{\mathcal{L}}{V} \left\langle \frac{\partial V}{\partial \theta} \right\rangle - \alpha \frac{\mathcal{L}}{\mathbf{s}} \left\langle \frac{\partial \mathbf{s}}{\partial \theta} \right\rangle \quad (5)$$

One application of gradients in brain simulation is their applicability in tuning of parameters. Multi-compartmental neurons in brain simulators are highly nonlinear systems with many parameters. The aforementioned ION neuron model was optimized using the Adam optimizer, to replicate a known target voltage trace. As a comparison, traditional evolutionary search (CMA-ES[6]) was also included. For the 17-parameter model, both methods require approximately the same number of iterations to converge. However, for this, CMA-ES relies on 20 times as much compute per iteration to estimate the gradients. Including a gradient system next to the regular system for simulation incurred a double penalty during simulation. Afterwards, only minor runtime increase per included parameter is observed (fig. 2E).

**Homeostatic Control** One advantage of the gradient system over externally calculated gradients, is the availability of gradients within the system itself. These can be used for *online* optimization of neurons: homeostatic control. This section will focus on the later. Assume an instantaneous error  $e(V, \mathbf{s})$ . For simplicity, this error function will usually be a single element of  $\mathbf{s}$ , which is then an integrated loss term as  $\mathbf{s}_0 = \int_0^t l(v, \mathbf{s})$  and with  $e(V, \mathbf{s}) = \mathbf{s}_0$ .

Now, we interpret gradient descent as a dynamical system, and include a forget fullness parameter  $\lambda$  and learning rate  $\alpha$ :

$$\dot{\theta} = -\alpha \frac{\partial e(\mathbf{s})}{\partial \mathbf{s}} \left\langle \frac{\partial \mathbf{s}}{\partial \theta} \right\rangle + \xi \Delta \theta \quad (6)$$

Notable, we can simulate, train and optimize using a regular forward-time differential equation solver. The forgetfulness parameter is needed to accommodate for the updated values of  $\theta$ , which are not reflected yet in  $\left\langle \frac{\partial \mathbf{s}}{\partial \theta} \right\rangle$  and to make sure the gradients don't explode for a long running simulation. Given appropriate selection of  $\alpha$ , this system is stable (see Methods).

## Discussion

Existing brain simulators can calculate gradients for neuron models. They are not designed for this tasks, yet the gradients of the neuron takes on similar enough form that we can trick a simulator in calculating it. This then enables much needed gradient-based optimization on neural models and beyond. Moreover, the gradient model did not rely on unphysical mechanisms like non-local communication, and could be fully expressed via diffusion and local computations; in other words: gradients are in theory calculable by biology itself.

Beyond model parameters, many *dynamical* plasticity processes are unknown within the cell. Using meta-learning, such processes can be estimated back from data. At the same time, gradient can be used for dynamical control inside a simulation.

It would be desirable if the method would extend to networks as well. However, the gradient can not jump between cells and multicellular networks still. This is not possible within existing simulators, and would require cooperation from the brain simulation software itself. However, even partial gradient here should provide enough insights to tune cells to correct behavior: exemplified by biology, which also tunes cells using only local information.

A more convenient programming API, in the form of Arbor-Pycat, was essential to building more complex models. For programming more complex brain models, NMODL interface is not enough.

Neural tuning often optimizes frequency, amplitude or symmetry of oscillations or spikes. These are measurable given a full trace of the cell, but not at an instant. Developing techniques for gradients in such simulation would truly enable the power of gradient-based tuning in an online setting. Structural plasticity is another topic which was not touch upon, but could have gradients as well, to truly decouple neurons from being ‘glass models’.

## Methods

In this section we explain how the gradient model is derived from the cable equations, and evaluation

of the approach. We start with a description of the cable equation as used in brain simulation software, followed by a short description of the *sensitivity equation*. We then combine these equations to form the gradient model. Then we discuss the stability of homeostatic mechanisms built on top of these gradients and why a forgetting parameter  $\lambda$  needs to be introduced. We end with the evaluation methods.

**Brain Simulation** Computational neuroscience seeks to gain knowledge about the brain by simulation and analysis of models of biological models, at the required level spatial and biophysical accuracy for the given research question.

The simplest possible equation to model a neuron is the integration of currents  $i$  over its capacitive membrane. This *transmembrane* current is usually the sum of individual modelled ionic channel currents. The current through each ionic channel are calculated from the cell’s voltage, channel internal state  $\mathbf{s}$  and system parameters  $\theta$ .

However, biological neurons, have an intricate spatial structure: Stereotypically, a single root (soma), an axon, and a branched dendritic tree. Modelling this accurately requires modelling the spatial structure of these neurons. In effect, beyond current influx and outflux over the cell membrane, we also model the *longitudinal* current along the branches of the neural structure (fig. 1A, blue). This is visible as a diffusion operator ( $\Delta_x$ ) in the voltage equations.

In modelling, these spatial trees are discretized into *segments*, leading to *multicompartmental* neural models. Each segment is treated as a tapered cylinder. The longitudinal diffusion term takes this into account by considering the change in surface area with respect to longitudinal distance ( $\frac{\partial S}{\partial x}$ ). Trivially,  $(\frac{\partial S}{\partial x}) = 2\pi R$  for a regular cylinder radius. Thus, we are left with the following *cable equation*[7, 8]

$$\dot{V} = \frac{\Delta_x V}{C_m R_l (\frac{\partial S}{\partial x})} - \frac{i(V, \mathbf{s}, \theta)}{C_m} \quad (7)$$

$$\dot{\mathbf{s}} = \mathbf{f}(V, \mathbf{s}, \theta) \quad (8)$$

**Brain Simulation Software** Biophysical realistic neurons are simulated using dedicated brain simu-

Pseudo-NMODL (Arbor dialect) Gradients Implementation

```

NEURON {
  SUFFIX dual
  NONSPECIFIC_CURRENT i
  USEIONS x1..M WRITE xd1..M
  RANGE s, theta, <math>\left\langle \frac{\partial V}{\partial \theta} \right\rangle, \left\langle \frac{\partial \mathbf{s}}{\partial \theta} \right\rangle
}
STATE {
  s ∈ ℝN    <math>\left\langle \frac{\partial V}{\partial \theta} \right\rangle ∈ ℝM
  theta ∈ ℝM <math>\left\langle \frac{\partial \mathbf{s}}{\partial \theta} \right\rangle ∈ ℝN \times M
}
INITIAL {
  <math>\left\langle \frac{\partial \mathbf{s}}{\partial \theta} \right\rangle = \mathbf{0}</math>
  <math>\left\langle \frac{\partial V}{\partial \theta} \right\rangle = \mathbf{0}</math>
}

DERIVATIVE d {
  <math>\left\langle \frac{\partial V}{\partial \theta} \right\rangle = \text{xd}</math>
  <math>\dot{\mathbf{s}} = \mathbf{f}(V, \mathbf{s}, \theta)</math>
  <math>\left\langle \frac{\partial \dot{V}}{\partial \theta} \right\rangle = -\frac{\partial i}{C_m \partial \theta} - \frac{\partial i}{C_m \partial V} \left\langle \frac{\partial V}{\partial \theta} \right\rangle</math>
  <math>-\frac{\partial i}{C_m \partial \mathbf{s}} \left\langle \frac{\partial \mathbf{s}}{\partial \theta} \right\rangle</math>
  <math>\left\langle \frac{\partial \dot{\mathbf{s}}}{\partial \theta} \right\rangle = \frac{\partial \mathbf{f}}{\partial \theta} + \frac{\partial \mathbf{f}}{\partial V} \left\langle \frac{\partial V}{\partial \theta} \right\rangle + \frac{\partial \mathbf{f}}{\partial \mathbf{s}} \left\langle \frac{\partial \mathbf{s}}{\partial \theta} \right\rangle</math>
}
BREAKPOINT {
  SOLVE d METHOD sparse
  i = i(V, s, theta)
  xd = <math>\left\langle \frac{\partial V}{\partial \theta} \right\rangle</math>
}

```

Figure 3: Implementation of the gradient system in NMODL interface.  $\text{xd}$  is a vector of ions. Some freedom of notation was allowed: NMODL does not support vectors or matrices. Instead, such objects should be read as written as single scalar values (i.e.  $\mathbf{s} = s_1, s_2 \dots s_N$ )

lation platforms, including NEURON[9], Arbor[8], EDEN[10]. These contain the necessarily patchwork of mechanism to define a neural model. A full mathematical model describing these does not exist.

Of great importance to the modeler is the interface used to describe the model to the simulator. NEURON and Arbor use the NMODL language to define mechanism dynamics, while EDEN is built around the NeuroML language. In Arbor, NMODL is compiled to a C++ *mechanism catalogue*, which then interfaces with a common Application Binary Interface (ABI).

The cable equation in eq. (7) is taken from the Arbor brain simulator, but the same equation is solved by NEURON or EDEN. On the programming side, these brain simulators allow the user to specify the functions  $i(V, \mathbf{s}, \theta)$  and  $\mathbf{f}(V, \mathbf{s}, \theta)$  using the NMODL or NeuroML languages, the rest is handled by the

simulator.

**Sensitivity Equation** Assuming general dynamical system  $\dot{x} = f(x, \theta)$ , we have the time derivative of the state-parameter gradient as the sensitivity equation ([11]):

$$\frac{d}{dt} \left\langle \frac{\partial x}{\partial \theta} \right\rangle = \frac{\partial f(x, \theta)}{\partial \theta} + \frac{\partial f(x, x)}{\partial \theta} \left\langle \frac{\partial x}{\partial \theta} \right\rangle \quad (9)$$

where we denote with  $\langle \cdot \rangle$  the state matrix of this new *gradient system*, for which we can explicitly solve using numerical integration.

**Gradients for Brain Models** The most obvious solution to calculate gradient for neural models is by automatic gradient calculation throughout the entire simulator[5].

$$\frac{dV}{d\theta} = \frac{d}{d\theta} \text{ODESolve} \left( \frac{dV}{dt} \right) \quad (10)$$

This does not work in practice: automatic gradient calculation is not possible through existing brain simulators. Writing an differentiable ODESolve function to handle brain models, would constitute to writing a new brain simulator from scratch, which is a long and costly effort. Instead, we implement gradients simulators by co-simulating the *gradient model* of a neuron, next to the neuron itself, in the simulator. This way we can leverage the development effort and optimization put into the simulators of problems of this specific kind.

Applying the sensitivity equation eq. (9) to the cable equation eq. (7), we obtain the gradient system for the cable cell: As such, we can now express a second *gradient model*, as:

$$\begin{aligned} \left\langle \frac{\partial \dot{V}}{\partial \theta} \right\rangle &= \frac{\Delta_x \left\langle \frac{\partial V}{\partial \theta} \right\rangle}{C_m R_l \left( \frac{\partial S}{\partial x} \right)} - \frac{1}{C_m} \frac{\partial i}{\partial \theta} \\ &\quad - \frac{1}{C_m} \frac{\partial i}{\partial V} \left\langle \frac{\partial V}{\partial \theta} \right\rangle - \frac{1}{C_m} \frac{\partial i}{\partial \mathbf{s}} \left\langle \frac{\partial \mathbf{s}}{\partial \theta} \right\rangle \end{aligned} \quad (11)$$

$$\left\langle \frac{\partial \dot{\mathbf{s}}}{\partial \theta} \right\rangle = \frac{\partial \mathbf{f}}{\partial \theta} + \frac{\partial \mathbf{f}}{\partial V} \left\langle \frac{\partial V}{\partial \theta} \right\rangle + \frac{\partial \mathbf{f}}{\partial \mathbf{s}} \left\langle \frac{\partial \mathbf{s}}{\partial \theta} \right\rangle \quad (12)$$

Notably, the longitudinal voltage-diffusion term led to a *gradient-diffusion* term in the gradient model. Diffusion of state variables is not expressible in NEURON or Arbor. Instead, we can use built-in diffusion of custom ions, for example in Arbor[12]:

$$\dot{c} = \frac{\beta \Delta_x}{\left( \frac{\partial S}{\partial x} \right)} c + i_c \quad (13)$$

by setting  $\beta = \frac{1}{C_m R_l}$  (in practice,  $\beta = 100/C_m R_l$  after unit conversion). In this way, we can calculate gradients for multicompartmental cells against the normal Arbor user API.

The resulting gradient system reflects a lot about the underlying system. In the case of neurons, we can express the gradient system as a ion-channel mechanism and a set of extra diffusive ions. Their dynamics can we derived by (automatic) gradient cal-

Soma (S/cm <sup>2</sup> )	Dendrite (S/cm <sup>2</sup> )
$g_{\text{leak}} = 1.3 \times 10^{-5}$	$g_{\text{leak}} = 1.3 \times 10^{-5}$
$g_{\text{CaL}} = 0.045$	$g_{\text{KCa}} = 0.220$
$g_{\text{Na}} = 0.030$	$g_{\text{CaH}} = 0.010$
$g_{\text{Kdr}} = 0.030$	$g_{\text{h}} = 0.015$
$g_{\text{K}} = 0.015$	
Axon (S/cm <sup>2</sup> )	Potential (mV)
$g_{\text{leak}} = 1.3 \times 10^{-5}$	$V_{\text{leak}} = 10$
$g_{\text{Na}} = 0.200$	$V_{\text{Ca}} = 120$
$g_{\text{K}} = 0.200$	$V_{\text{Na}} = 55$
	$V_{\text{K}} = -75$
	$V_{\text{h}} = -43$

Table 1: Initial parameters for inferior olivary cell model

ulation from the existing neuron model. A template NMODL file implementing the gradient model is shown in fig. 3.

**Homeostatic Control Stability** Consider a passive neuron model with a target potential and leak reversal potential as parameter

$$i = g_l (V - E_{\text{leak}}) \quad \dot{s} = \frac{1}{2} (V - E_{\text{target}})^2 \quad (14)$$

$$\theta = E_{\text{leak}} \quad e = s_0 \quad (15)$$

Leading to the following nonlinear system of PDEs for a single linear neuron with no varying radius (or equivalently,  $R_l < \infty$ ), where we have included a gradient-forgetting parameter  $\lambda$  to prevent stability problems (as will be shown next).

$$\dot{V} = \frac{\Delta_x V}{2\pi R C_m R_l} - \frac{g_l (V - E_{\text{leak}})}{C_m} \quad (16)$$

$$\left\langle \frac{\partial \dot{V}}{\partial \theta} \right\rangle = \frac{\Delta_x \left\langle \frac{\partial V}{\partial \theta} \right\rangle}{2\pi R C_m R_l} + \frac{g_l}{C_m} \left( 1 - \left\langle \frac{\partial V}{\partial \theta} \right\rangle \right) \quad (17)$$

$$\dot{\theta} = -\alpha \left\langle \frac{\partial \mathbf{s}}{\partial \theta} \right\rangle \quad (18)$$

$$\left\langle \frac{\partial \dot{\mathbf{s}}}{\partial \theta} \right\rangle = -\lambda \left\langle \frac{\partial \mathbf{s}}{\partial \theta} \right\rangle + (V - E_{\text{target}}) \left\langle \frac{\partial V}{\partial \theta} \right\rangle \quad (19)$$

After the initial transient we obtain  $\langle \frac{\partial V}{\partial \theta} \rangle = 1$ . Without loss of generality, we can set  $E_{\text{target}} = 0$ . If we now apply a spatial sinusoidal perturbation  $V \propto \sin(\omega x)$ , we obtain the linear system.

$$\frac{d}{dt} \begin{pmatrix} V \\ \langle \frac{\partial s}{\partial \theta} \rangle \\ E_{\text{leak}} \end{pmatrix} = \begin{pmatrix} \frac{-g_l}{C_m} - \frac{\omega^2}{2\pi R C_m R_l} & 0 & \frac{g_l}{C_m} \\ 1 & -\lambda & 0 \\ 0 & -\alpha & 0 \end{pmatrix} \begin{pmatrix} V \\ \langle \frac{\partial s}{\partial \theta} \rangle \\ E_{\text{leak}} \end{pmatrix} \quad (20)$$

and resulting Routh–Hurwitz stability criterion

$$\alpha < \frac{(\pi C_m^2 R R_l \lambda \omega^2 + 2g_l \lambda) (\pi C_m^2 R R_l \omega^2 + 2C_m \lambda + 2g_l)}{4C_m g_l} \quad (21)$$

which has a lower bound as  $\alpha < \lambda \left( \lambda + \frac{g_l}{C_m} \right)$  in the case  $\omega = 0$  (or a single point neuron). In other words: to have stable online learning, the gradient needs to forget. Beyond this, spatial perturbations do not make the system more unstable. The same analysis can be repeated by adding a  $\beta_\theta \Delta_x \theta$  diffusion term to the theta equation, where again spatial perturbations do not lead to a more unstable system.

**Axon model** The Hodgkin-Huxley model was implemented in NMODL, as well as its gradient system using eq. (12). The SymPy library was used to implement gradient-calculation from model to gradient system to generate NMODL code. An axon was defined of 11 compartments, using the resulting mechanism. A current pulse was applied at  $t=200\text{ms}$  and multiplied by the parameter  $\theta = w$  before being injected into one end of the axon.

**Arbor-Pycat Library** Crucial in the method is availability of gradients for the current and ode system, greatly amplified by automatic gradients calculation systems - eg. JAX. To ease implementation, a python wrapper around the C mechanism ABI was written that exposed the mechanism internals as numpy-style buffers, allowing JAX to work with it. This is released as a separate package.

**IO model** A modified version[13] of the de Gruijl model[14] was implemented in Arbor-Pycat. The

morphology of mouse IO neuron C4A was used[15]. After discretization, it contains 4 axonal, 15 dendritic and 2 somatic compartments. Initial parameters are listed in Table 1. Optimization was performed against the loss-function:

$$\mathcal{L} = \frac{1}{T} \int_0^T (v(t) - \hat{v}(t))^2 dt \quad (22)$$

The Adam optimizer with learning rate  $10^{-3}$  was used. This was compared to the the CMA-ES algorithm with population size 20 and initial  $\sigma = 0.1$ . Initial parameters are listed in table 1.

**Hardware** AMD Ryzen 9 3900X 12-Core processor and NVIDIA RTX 6000 GPU

**Acknowledgments** This paper is partially supported by the European-Union Horizon Europe R&I program through projects SEPTON (no. 101094901) and SECURED (no. 101095717) and through the NWO - Gravitation Programme DBI2 (no. 024.005.022). The RTX6000 used for this research was donated by the NVIDIA Corporation.

## References

- [1] Quentin JM Huys, Misha B Ahrens, and Liam Paninski. Efficient estimation of detailed single-neuron models. *Journal of neurophysiology*, 96(2):872–890, 2006.
- [2] Willem AM Wybo, Jakob Jordan, Benjamin Ellenberger, Ulisses Marti Mengual, Thomas Nevian, and Walter Senn. Data-driven reduction of dendritic morphologies with preserved dendrosomatic responses. *Elife*, 10:e60936, 2021.
- [3] Werner Van Geit, Michael Gevaert, Giuseppe Chindemi, Christian Rössert, Jean-Denis Courcol, Eilif Benjamin Muller, Felix Schürmann, Idan Segev, and Henry Markram. Bluepyopt: Leveraging open source software and cloud infrastructure to optimise model parameters in neuroscience. *Frontiers in Neuroinformatics*, 10



- (17), 2016. ISSN 1662-5196. doi: 10.3389/fninf.2016.00017.
- [4] Pedro J Gonçalves, Jan-Matthis Lueckmann, Michael Deistler, Marcel Nonnenmacher, Kaan Öcal, Giacomo Bassetto, Chaitanya Chintaluri, William F Podlaski, Sara A Haddad, Tim P Vogels, et al. Training deep neural density estimators to identify mechanistic models of neural dynamics. *Elife*, 9:e56261, 2020.
- [5] Ilenna Simone Jones and Konrad Paul Kording. Efficient optimization of ode neuron models using gradient descent. *arXiv preprint arXiv:2407.04025*, 2024.
- [6] Nikolaus Hansen, Youhei Akimoto, and Petr Baudis. CMA-ES/pycma on Github. Zenodo, DOI:10.5281/zenodo.2559634, February 2019. URL <https://doi.org/10.5281/zenodo.2559634>.
- [7] Michael L Hines and Nicholas T Carnevale. The neuron simulation environment. *Neural computation*, 9(6):1179–1209, 1997.
- [8] N. Abi Akar, B. Cumming, V. Karakasis, A. Küsters, W. Klijn, A. Peyser, and S. Yates. Arbor — A Morphologically-Detailed Neural Network Simulation Library for Contemporary High-Performance Computing Architectures. In *2019 27th Euromicro International Conference on Parallel, Distributed and Network-Based Processing (PDP)*, pages 274–282, feb 2019. doi: 10.1109/EMPDP.2019.8671560.
- [9] Nicholas T Carnevale and Michael L Hines. *The NEURON book*. Cambridge University Press, 2006.
- [10] Sotirios Panagiotou, Harry Sidiropoulos, Dimitrios Soudris, Mario Negrello, and Christos Strydis. Eden: A high-performance, general-purpose, neuroml-based neural simulator. *Frontiers in neuroinformatics*, 16:724336, 2022.
- [11] Thomas Hakon Gronwall. Note on the derivatives with respect to a parameter of the solutions of a system of differential equations. *Annals of Mathematics*, 20(4):292–296, 1919.
- [12] Nora Abi Akar, John Biddiscombe, Benjamin Cumming, Marko Kabic, Vasileios Karakasis, Wouter Klijn, Anne Küsters, Alexander Peyser, Stuart Yates, Thorsten Hater, Brent Huisman, Espen Hagen, Robin De Schepper, Charl Linssen, Harmen Stoppels, Sebastian Schmitt, Felix Huber, Max Engelen, Fabian Bösch, Jan-nik Luboeinski, Simon Frasch, Lukas Drescher, and Lennart Landsmeer. Arbor library v0.9.0, November 2023. URL <https://doi.org/10.5281/zenodo.8233847>.
- [13] Mario Negrello, Pascal Warnaar, Vincenzo Romano, Cullen B Owens, Sander Lindeman, Elisabetta Iavarone, Jochen K Spanke, Laurens WJ Bosman, and Chris I De Zeeuw. Quasiperiodic rhythms of the inferior olive. *PLoS computational biology*, 15(5):e1006475, 2019.
- [14] Jornt R De Gruijl, Paolo Bazzigaluppi, Marcel TG de Jeu, and Chris I De Zeeuw. Climbing fiber burst size and olivary sub-threshold oscillations in a network setting. *PLoS computational biology*, 8(12):e1002814, 2012.
- [15] Nora Vrieler, Sebastian Loyola, Yasmin Yarden-Rabinowitz, Jesse Hoogendorp, Nikolay Medvedev, Tycho M Hoogland, Chris I De Zeeuw, Erik De Schutter, Yosef Yarom, Mario Negrello, et al. Variability and directionality of inferior olive neuron dendrites revealed by detailed 3d characterization of an extensive morphological library. *Brain Structure and Function*, 224(4):1677–1695, 2019.